[156] *Artificially Layered Materials,* Ivan K. Schuller, World Material Congress, 1988
Chapter 7 in "Science of Advanced Materials", H. Wiedersich and M.Meachii, eds.
(ASM International, Materials Park, Ohio, 1990), pg. 225.

Artificially Layered Materials

Ivan K. Schuller
Physics Department - B-019
University of California, San Diego
La Jolla, CA 92093

Abstract

Artificially Layered Materials are used as model systems to test theoretical ideas regarding a variety of phenomena including thin films, interfacial, proximity, coupling and superlattice effects. I describe here the preparation, characterization and physical properties of Artificially Layered Materials and show some examples which characterize each one of the effects mentioned above. I also outline some of the unsolved problems which are currently being researched.

I. Introduction

The study of novel artificially-layered materials is a field which has received an ever increasing attention in the last 10-20 years. This attention originates from a symbiotic relationship between basic researchers who are interested in studying new and unusual materials and technologists who develop ever more sophisticated devices which allow control of growth at the atomic level. This field includes the development of metastable materials, thin films, small particles,composites, amorphous materials, ceramics, etc.

In particular, the growth of multilayered films with individual layer thicknesses approaching interatomic distances, is receiving attention by a large number of research groups. Much interesting physics and material science has been discovered in these artificially layered materials. These include the observation of quantum wells and phonon folding in semiconductor multilayers, anomalous elastic constants, dimensional behavior, and coupling effects in metallic multilayers. One important area which is receiving ever increasing attention is the use of these materials as model systems for naturally occurring materials, for instance, high-temperature superconductors. Many applications are also being pursued including mirrors for soft x-rays and neutrons, high critical current superconductors, voltage tunable Josephson radiators, etc.

We will describe here representative aspects of this field ***using only examples from our own work***. Clearly, in such a brief review it is impractical to attempt a review of all the literature. For this the reader is referred to several recent exhaustive reviews of the subject.[1-4] This review was completed at the end of 1988.

II. Preparation.

The preparation of layered materials has been increasing in sophistication especially with the advent of deposition techniques which allow preparation of high melting point, refractory, or ceramic materials in ultrahigh vacuum (~ 10^{-11} Torr). In many cases such sophisticated (and expensive) techniques are not necessary especially if the phenomena being studied are not affected by small amounts of contamination, as is the case for metals. Moreover, the relevant quantity which controls the contamination is the deposition rate divided by the pressure (***during*** deposition) and not the absolute, ultimate vacuum. Therefore, in many cases, for instance, sputtering, it is desirable to increase the deposition rate as opposed to improving the ultimate vacuum.

One technique which has received considerable attention, for the growth of semiconductors and more recently for metals, is Molecular Beam Epitaxy (MBE). In this technique several molecular beams, prepared either by thermal evaporation or electron beam bombardment, are aimed at a heated substrate. The rates of the individual sources are controlled either by controlling the temperature (as for Knudsen cells) or using thickness monitors in a feedback mode (as for electron beam gun evaporators). Fig. 1 shows a top view of such an apparatus manufactured by The Riber Division of Instruments SA, Inc. All sources are located on the periphery of a circle aimed at a centrally located heated substrate. Simultaneously, during deposition, an electron beam is reflected from the sample at low angles, thus allowing *in-situ* diffraction studies of the growing film.

A variety of other growth techniques have also been applied to the preparation of multilayers. These include sputtering and ion beam deposition. In all cases the preparation of the layered material is done by alternately depositing materials on a heated substrate.

III. Characterization.

The characterization of these materials has received much attention.[5] To date most structural characterization techniques are only able to determine the structure of the materials semiquantitatively. Further studies are needed to ascertain the degree of interfacial roughness, interdiffusion, crystallinity, etc. Each technique has a number of advantages and disadvantages and therefore, in order to elucidate the structure of a material it is necessary to apply a full battery of tests in a complimentary fashion.

Fig. 2 shows an electron micrograph of a vertical microcleavage cross section of a tungsten-carbon Fabry-Perot structure.[6] This type of cross section is very useful in studying relative thicknesses of the constituents and in feeding back into the growth process. It should be realized that this micrograph only determines the ***averaged*** structure along the electron path (parallel to the layers in this case). The effect of this averaging is not well-understood and presently under study.

Chemical composition in the perpendicular direction to the substrate can be obtained using a number of surface techniques in conjunction with ion milling. Fig. 3 shows the ion mill Auger depth profile of a Nb/Cu multilayer. The Nb concentration is out of phase with the Cu concentration and oscillates in a periodic fashion. However finite escape depths for electrons and intermixing caused by the ion bombardment limit the application of these techniques in practice to thicknesses larger than 50 Å. More sophisticated techniques, including the deconvolution of the finite electronic escape depth are currently being pursued.

One characterization technique which is non-destructive and readily available in most laboratories is X-ray diffraction. The most often used diffraction technique is the so called θ-2θ diffraction with the scattering vector perpendicular to the film surface. In this fashion, the structure parallel to the scattering vector (i.e. perpendicular to the film surface) is obtained. Since in X-ray diffraction the ***intensity*** of the scattered X-ray is detected, the phase information is lost and therefore it is not possible to directly invert the intensities to obtain the structure. Models are needed!! In the models, a number of adjustable parameters such as variations in layer thickness, lateral roughness, interdiffusion, etc. must be included in order to obtain even qualitative agreement with the experimental data. Presently a large amount of effort is devoted to develop proper models which can explain the diffraction data quantitatively. The main difficulty, lies in the fact that many types of disorder are present which imply a large number of unknown parameters ***a-priori.*** It is therefore important to study further the growth processes at the atomic level by developing theoretical and numerical methods which hopefully will clarify the role and importance of the various parameters.

Conventionally the X-ray diffraction spectrum is divided into two ranges: "low" angle (below ~ 10 degrees) and "high" angle (above 10 degrees). In principle, the low angle data gives directly the Fourier transform of the composition profile. In practice, however, so-called ***dynamical corrections*** complicates considerably the application of ***kinematic*** X-ray diffraction to the small angle region.[7] More sophisticated methods, including intrinsically dynamical theories such as the Fresnel formulation, also need ***a-priori*** knowledge of parameters, such as optical constants in the appropriate wavelength regime, which are not known in thin films.

High-angle superlattice data is obtained ***only*** if a coherent stacking of the atomic planes is present. For instance, small amounts of continuous fluctuations in layer thickness completely washes out high angle multilayer peaks in (crystalline) Pb/(amorphous) Ge multilayers.[8] Fig. 4 shows high angle diffraction spectra from Nb(34 Å)/Cu (34 Å) multilayers.[9] In this region of scattering angle, thick Nb and thick Cu layers only show one peak, each characteristic of the Nb(110) and Cu(111) atomic planes. The separation of the new peaks (shown in the figure) is only given by the periodicity of the multilayer, whereas their intensity is governed by the arrangement of atoms within one period. Multilayers that exhibit this type of ***coherent*** stacking are denoted as ***superlattices*** since an additional periodicity in addition to the atomic periodicity is present.

A large number of effects exist which may destroy the presence of superlattice diffraction peaks. These include variation in thickness from layer to layer, roughness, interdiffusion, formation of interfacial alloys, and so on. The determining factors for superlattice growth are not established at the present time. They probably include a variety of factors, such as wetting, lattice matching, thermodynamic phase diagrams and growth conditions, that vary from system to system.

IV. Physical Properties

The physical properties of multilayered materials can be classified conveniently depending on the number of layers required for the observation of each effect. Since multilayered films consist of stacks of single layers the simplest phenomena which can be observed are ***single film effects.*** The proximity of two physically dissimilar films (for instance, superconducting and normal metals) gives rise to ***proximity effects.*** The fact that in layered materials a large number of interfaces are present is the cause for ***interfacial effects***. The coupling of a physical property, such as the magnetization, across a different type of materials (for instance a non-magnetic one) gives rise to ***coupling effects*** and it only requires the presence of three films. The one effect which depends on the periodic nature of the multilayer is the so called ***superlattice effect.*** This has only been observed in a few cases, the earliest being the observation of phonon folding in GaAs/AlAs semiconductor superlattices.[10] Although in many cases the multiple nature of the stack is not strictly necessary for the observation of a particular phenomenon the presence of a multiple stack has considerable technical advantages.

I will give here a few examples **from our own work** to illustrate some of these effects in metallic superlattices.

a. Single Film Effects

Because the multilayer is made up from a collection of thin films in many cases this is the only effect observed. Although this effect does not require a multilayer, in practice, in many cases, these effects are more conveniently studied in a multilayer. The reason is that by preparing a multilayer it is possible to avoid a large number of questions regarding, for instance, surface contamination which distorts many studies made on single films.

An example of a single film effect is the dependence of magnetization of Ni as a function of thickness observed in Ni/Mo multilayers (fig. 5).[11] The magnetization mostly changes with Ni thickness and is only slightly affected by the presence of Mo. The detailed reason for this dependence has not been ascertained, however, it is thought to be related to the presence of magnetic dead layers at the interface between Mo and Ni. A model calculation assuming two dead layers at the interface explains the qualitative trend of the data as shown by the dashed line in the figure.

Other single film effects include notably the dependence of the ***parallel*** electrical resistivity as a function of layer thickness (t), as shown in Figure 6.[12] The electrical resistivity increases linearly with 1/t until it reaches a resistivity corresponding roughly to the minimum metallic conductivity[13] of ~ 150 μΩcm and then it saturates. This dependence is due to interfacial scattering and it implies that the resistivity originates from boundary scattering and has been observed much earlier in single metal films. These measurements imply that the electrons are confined mostly to move ***within*** one layer. Therefore, effects which depend on having extended electronic states perpendicular to the layers will be very hard to observe.

b. Interfacial Effects

Interfacial effects are produced because layered materials possess a large number of interfaces. Although a number of experiments have searched for the presence of interfacial electronic states these have not been observed.

The interface, however, has been shown to posses a drastic effect on the dependence of the crystallization temperature in amorphous semiconductors. Figure 7 shows the dependence of the crystallization temperature in amorphous semiconductors. Figure 7 shows the dependence of the crystallization temperature T_x of amorphous Ge in Pb/Ge multilayers.[14] T_x is found to depend on the thicknesses of germanium (d_{Ge}) (Fig. 7a), of lead (d_{Pb}) (Fig. 7b) and on the rocking curve width $\Delta\omega$ of the crystalline lead (Fig. 7c). The dependence as a function of $\Delta\omega$ implies that the germanium crystallization starts at the interface because the better the texture of lead, the lower the value of T_x, since the Pb film acts as a template for the initial Ge nucleus. An improved Pb texture facilitates the crystallization of the amorphous Ge thereby decreasing the crystallization temperature. The dependences as a function of d_{Pb} and d_{Ge} can also be understood as due to an interfacially initiated crystallization together with the energetics of crystallization.

Interfacial effects have also been found in the dependence of the magnetic anisotropy in normal/magnetic superlattices and in particular the linear dependence of the anisotropy as a function of 1/t (t = thickness of the film) showing that the changes in the anisotropy originate from the interface.[15]

c. Proximity Effects

The most fruitful studies of proximity effects have been studied in conventional superconductor/normal metal sandwiches.[16] Since the relevant length (coherence length) in conventional superconductors and normal metals is very long ($\geq$100 Å) it was relatively easy to design experiments to study proximity effects, even in single sandwiches. Moreover, the extensive theoretical studies not only allowed qualitative observations, but detailed quantitative comparisons between experiment and theory. Very similar studies have also been performed in conventional superconductor/normal metal multilayers.

Fig. 8 shows the dependence of the critical temperature (T_c) of Nb as extracted from Nb/Ge multilayers,[18] Nb/Cu multilayers[19] and single Nb[20] films. The Nb T_c is extracted from the Nb/Ge data by extrapolating the multilayer data as a function of Ge thickness (d_{Ge}) to d_{Ge} > 0. The T_c from the Nb/Cu data is obtained using the experimentally measured values together with the de Gennes- Werthammer theory of proximity effect.[16-17] The single film data is from actual experimental measurements.

The comparison of these three sets of data beautifully illustrates the technical advantages multilayers have, even for the study of single film effects. The single Nb film data can only be understood by invoking the presence of an uncontrollable layer of oxide on the Nb surface. Since the thickness of this oxide layer and ***the type of oxide*** possibly depends on details of growth conditions, it is very difficult to ascertain unequivocally the thickness dependence of T_c of a single Nb layer.

The two sets of multilayer data are in reasonable agreement and show that the application of proximity effect theory to Nb/Cu multilayers can account for part of the changes in T_c. The additional intrinsic thickness dependence of the Nb T_c (in both Nb/Cu and Nb/Ge) is thought to originate from mean free path smearing of the density of states at the Fermi surface.

d. Dimensional and Coupling Effects

The dimensionality of a film can be tuned in a convenient fashion by coupling through an unlike film. For instance, a stack of two dimensional (i.e. $t < \xi$) superconducting films will behave as two dimensional (2D) if they are separated by thick semiconductor layers. As the separator thickness is decreased the superconducting layers progressively couple together and exhibit progressively more three dimensional (3D) character.

One property which is strongly affected by dimensionality is the superconducting upper critical field H_{c2}. The upper critical field of a 3D anisotropic superconductor is given by:

$$H_{c2\parallel}(T) = \frac{\phi_o}{2\pi} \frac{1}{\xi_\parallel(T)\, \xi_\perp(T)} \qquad (1)$$

and $$H_{c2\perp}(T) = \frac{\phi_o}{2\pi} \frac{1}{\xi_\parallel^2(T)} \qquad (2)$$

where $\xi_\parallel$ (T) and $\xi_\perp$ (T) are the parallel and perpendicular temperature dependent coherence lengths and ϕ_o the flux quantum. A single superconducting film with dimension $t < \xi_\perp(T)$, (i.e. two dimensional) has an upper critical field

$$H_{c2\parallel}(T) = \frac{\phi_o}{2\pi} \frac{1}{t} \frac{1}{\xi_\parallel(T)} \qquad (3)$$

Therefore, a comparison of equation (1) and (3) shows that the main distinguishing feature between 2D and 3D behavior is the temperature dependence of $H_{c2\|}$. Since $\xi \alpha (T - T_c)^{-1/2}$; in 3D, $H_{c2\|}$ depends linearly on $(T-T_c)$ and in 2D it has a square root like dependence. The way to engineer this behavior into a multilayer film is to build a set of 2D superconducting films ($t_s < \xi$) separated by normal metals[21] or semiconductors.[18,22]

A single 3D Nb film shows typical linear behavior in $H_{c2\|}$ (T) as shown in fig (9a). A single 2D Nb film on the other hand shows a typical square root like behavior in $H_{c2\|}$ (T). The relevant quantity which determines the dimensionality of a multilayered superconductor is the thickness of the normal metal separator. If this separator is thick (compared to $\xi_\perp$ (T)), the stack behaves as a set of single 2D films, if the separator is thin (compared to $\xi_\perp$(T)), the multilayer exhibits 3D behavior.

Since $\xi_\perp$ diverges strongly as a function of the temperature close to T_c, $\xi_\perp$ (T) may be larger than the thickness of the normal metal separator, and therefore the behavior is 3D. As the temperature is reduced the coherence length decreases below the normal metal thickness, the superconducting layers decouple and behave as a stack of 2D films. This phenomenon known as "dimensional crossover"[22] is illustrated in figure (9c) for Nb/Cu multilayers where close to T_c the layers are coupled and the behavior is 3D (i.e. $H_{c2\|}$ is linear). At low temperatures the layers decouple and the behavior becomes 2D like (i.e. square root). This crossover occurs as expected roughly where $\xi_\perp (T_x) \sim d_{Cu}/2$ in Nb/Cu superlattices.[21]

The coupling is also dependent on the ratio of the density of states of the normal metal to superconductor.[23] Fig. 10 shows the effect the density of states ratio has on the dimensional crossover. The coupling progresses from a narrow range of 3D behavior close to T_c in Nb/Ge[22] to a progressively wider 3D range in Pb/Ge[24] and Nb/Cu,[21] as expected since the density of states ratio is increasing progressively in going from Nb/Ge to Pb/Ge and to Nb/Cu. The angular dependence of the critical field has also been studied and found to exhibit characteristic behavior of the dimensional transition.[21] Similar behavior has also been obtained in naturally occurring superlattices such as the recently discovered high temperature oxide superconductors.[25]

A variety of coupling effects have also been observed in magnetic multilayers including indirect RKKY coupling in Ni/Cu[26] and Gd/Y[27] and spiral magnetism in Dy/Y[28] superlattices.

c. Superlattice Effects

These type of effects depend on the existence of the new periodicity imposed by the layering. The first observations of such an effect was the so called "phonon folding" effect in GaAs/AlAs superlattices.[10] Much effort has gone into the observation of similar effects in the electronic properties of metallic superlattices. To date, the predicted minigaps in the electronic density of states in normal metals or the presence of states in the gap for superconductors have not been observed.[29] The reason for their absence is not clear but they may be related to strong interfacial scattering as implied by the dependence of resistivity on layer thickness.[12]

Magnetic/normal metal superlattices exhibit superlattice effects due to magnetic dipolar coupling across the normal metal.[30] Qualitatively it is expected that an isolated thin film has one surface mode which has to evolve in a continuous fashion into the surface and bulk modes present in a bulk ferromagnet. The details of this dependence, the magnetic field and wavevector dependences and coupling to light have been calculated theoretically.[31,32] The basic idea that emerges is that as the magnetic layers are brought closer together (i.e. smaller normal metal separator) the discrete magnons spread into bands and the light couples stronger to the bottom of the band. This is shown schematically in figure 11.

We have studied the behavior of the magnon spectra for three different series of samples of Mo/Ni superlattices.[30] Figure 12 shows the magnetic field dependence of the magnon frequency for selected samples. The theoretical curves are obtained from theoretical fits to experiment using only the saturation magnetization as an adjustable parameter. The saturation magnetization obtained from these fits is in agreement with independently measured saturation magnetizations using SQUID magnetometry. The wavevector dependence of the modes has also been studied and found to be in excellent agreement with theoretical prediction.

V. Conclusions

Artificially layered materials are ideal model systems for the study of a wide variety of physical phenomena including unusual behavior in their superconducting, magnetic, mechanical and transport properties. In many cases, precise theoretical predictions have been verified in detail. In other cases, despite considerable effort in a number of laboratories, many predicted phenomena have not been observed. In some cases, unexpected phenomena also occur. One notable example being the anomalous elastic behavior observed at short superlattice wavelengths.[33] One of the most important and intensive areas of current research is the study of disorder, interfacial roughness, interdiffusion, etc. and its effect on the structural probes used to characterize superlattices. The study of the effect of all these types of disorder should also be included in theoretical studies of physical phenomena in order to obtain quantitative agreements between theory and experiment.

VI. Acknowledgements

I would like to thank my collaborators over many years of research which have made all the research described here possible. This work was supported by the U.S. Department of Energy under Grant # DE FG03-87ER-45332 and the Office of Naval Research under Contract # N00014-88K-0480.

References

1. See various articles in "Synthetic Modulated Structures", L.L. Chang and B.C. Giessen, eds., Academic Press, Inc., Orlando (1985).
2. See various articles in "Interfaces, Superlattices and Thin Films", J.D. Dow and I.K. Schuller, eds., Materials Research Society Publishers, Vol. 77, Pittsburgh (1987).
3. For recent reviews, see "Physics, Fabrication and Applications of Multilayered Structures", P. Dhez and C. Weisbuch, eds. (In Press)
4. See various articles in "Multilayers: Synthesis, Properties and Non-Electronic Applications", T.W. Barbee Jr., F. Spaepen and L. Greer, eds., Materials Research Society Publishers, Vol. 103 (1988).
5. See for instance, D.B. McWhan, Chapter II in reference 1, ibid, pg. 43 and Chapter in ref. 3, ibid.
6. Y. Lêpetre et al., SPIE Proc. 563, 2158 (1985).
7. See for instance, A. Guinier, "X-ray Diffraction in Crystals, Imperfect Crystals and Amorphous Bodies", W. Freeman, San Francisco (1963).
8. J.-P. Locquet et al., in ref. 4, ibid, pg. 211.
9. I.K. Schuller, Phys. Rev. Lett. 44, 1597 (1980).
10. C. Colvard, R. Merlin, M.V. Klein and A.C. Gossard, Phys. Rev. Lett. 45, 298 (1980).
11. M.R. Khan, P.Roach and I.K. Schuller, Thin Solid Films 122, 183 (1985).
12. T.R. Werner et al., Phys. Rev. B. 26, 2224 (1982).
13. A. Joffe and A. Reggel, Prog. Semicond. 4, 237 (1960).
14. W. Sevenhans et al., Phys. Rev. B. 38, 4974 (1988).
15. P.F. Garcia, A.D. Meinhaldt and A. Suna, Appl. Phys. Lett. 47, 178 (1985).
16. For a review, see G. Deutcher and P.D. de Gennes in "Superconductivity", R.D. Parks, ed., Marcel Dekker Inc., New York (1969), pg. 1005.
17. For a review, see A. Gilabert, Ann. Phys. 2, 203 (1977).
18. S.T. Ruggiero, Ph.D. Thesis, Stanford University (1982), unpublished.

19. I. Banerjee et al., Sol. St. Comm. 41, 805 (1982).

20. S.A. Wolf, J.J. Kennedy and M. Nisenoff, J. Vac. Scie. Technol. 13, 145 (1976).

21. C.S.L. Chun et al., Phys. Rev. B. 29, 4915 (1984).

22. S.T. Ruggiero, T.W. Barbee Jr., and M.R. Beasley, Phys. Rev. B. 26, 4894 (1982).

23. S. Takahashi and M. Tachiki, Phys. Rev. B. 33, 4620 (1986).

24. J.-P. Locquet et al., IEEE Trans. Magn. MAG-23, 1393 (1987).

25. See for instance, various articles in "Proceedings of the International Conference on High Temperature Superconductors and Materials and Mechanisms of Superconductivity", J. Muller and J.L Olsen, eds., North Holland Amsterdam (1988).

26. W.S. Zhou et al., Physica 108B, 953 (1981).

27. J. Kwo et al., Phys. Rev. Lett. 55, 1402 (1985).

28. M.B. Salamon et al., Phys. Rev. Lett. 56, 259 (1986).

29. A.P. van Gelder, Phys. Rev. 181, 787 (1969).

30. A. Kueny et al., Phys. Rev. B. 29, 2879 (1984).

31. P. Grunberg and K. Mika, Phys. Rev. B. 27, 2955 (1983).

32. R.E. Camley, T.S. Rahman and D. Mills, Phys. Rev. B. 27, 261 (1983).

33. For a brief review, see I.K. Schuller in "1985 Ultrasonics Symposium", B.R. McAvoy, ed., IEEE Publishers (1985), pg. 1093.

Figure Captions

Fig. 1 Schematic diagram (top view) of a Riber, Inc. MBE System used for the preparation of high melting point refractory materials. The diagram shows two electron beam guns with quartz crystal and optical thickness controllers and three Knudsen Cells. All sources are located on the perimeter of a circle ("evaporation circle") and are aimed vertically at the heated substrate which is located at the center of the evaporation circle, above the sources.

Fig. 2 Electron micrograph of a WC Fabry-Perot structure showing the Si substrate, a thick (270 Å) C layer, a W (16 Å)/C (16 Å) multilayer, another thick (480 Å) C layer, followed by an additional W (16 Å)/C (16 Å) multilayer and capped by a C (170 Å) layer.

Fig. 3 Ion Mill Auger spectrum for a Nb (65 Å)/Cu (65 Å) multilayer, showing that the Nb and Cu concentrations oscillate out of phase.

Fig. 4 High angle θ-2θ X-ray diffraction from a Nb (34Å)/Cu (34Å) superlattices exhibiting superlattice peaks. Note, that the "central" peak is absent, unlike in GaAs/AlAs superlattices. This is due to the fact that the lattice spacing varies perpendicular to the layers.

Fig. 5 Saturation magnetization as a function of Ni thickness in Ni/Mo superlattices. The dashed line is a fit assuming two dead layers at the Ni/Mo interface.

Fig. 6 Low temperature (20 K) electrical resistivity for equal layer thickness Nb/Cu superlattices as a function of 1/t (t = layer thickness). The 1/t dependence due to interfacial electronic scattering is limited by the "maximum metallic resistivity" at small thicknesses.

Fig. 7 Ge crystallization temperature T_x as a function of Ge thickness (d_{Ge}), Pb thickness (d_{Pb}) and Pb texture ($\Delta\omega$). These dependences imply that the crystallization is initiated at the interface.

Fig. 8 Superconducting transition temperature (T_c) of Nb versus 1/t extracted from Nb/Ge multilayers ( ), Nb/Cu superlattices (o) and single Nb films (Δ).

Fig. 9 Upper critical field of (a) 3D Nb (8500 Å) film, (b) 2D Nb (191 Å) film and a Nb (172 Å)/Cu (333 Å) superlattice showing dimensional crossover. Perpendicular field (o) and parallel field (x). All films are covered by a thick (1500 Å) Cu to eliminate surface superconductivity.

Fig. 10 Normalized parallel upper critical field for Nb (65 Å)/Ge (35 Å) multilayer (+), Pb (140 Å)/Ge (20 Å) multilayer (o) and Nb (172 Å)/Cu (333 Å) superlattices ( ), showing the mean free path dependence of the dimensional crossover.

Fig. 11 Schematic dependence of the magnon frequency as a function of normal metal thickness in magnetic/normal superlattices. The density of dashed lines in the "band" of modes is illustrating that the light couples stronger to the bottom of the band. The arrows indicate the three series of experiments performed in Ni/Mo superlattices.

Fig. 12 Magnon frequency versus magnetic field for

a) d_{Ni} = 100 Å, d_{Mo} = 300 Å.
b) d_{Ni} = 100 Å, d_{Mo} = 100 Å.
c) d_{Ni} = 138 Å, d_{Mo} = 46 Å.
d) d_{Ni} = 250 Å, d_{Mo} = 750 Å.
e) d_{Ni} = 5000 Å, d_{Mo} = 5000 Å.
f) d_{Ni} = 540 Å, d_{Mo} = 180 Å.

The solid line shows a theoretical fit as explained in the text.

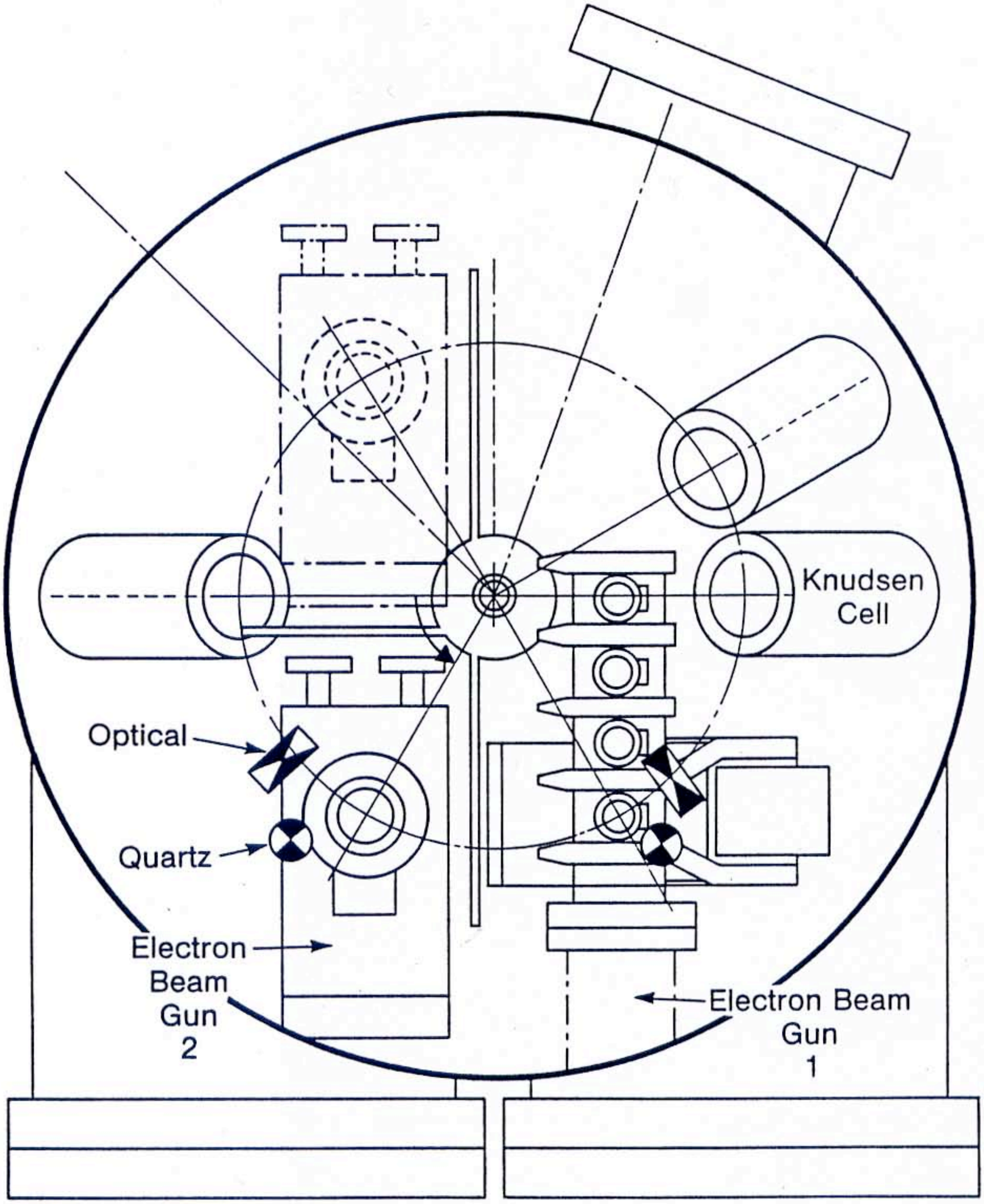

Knudsen Cell
Optical
Quartz
Electron Beam Gun 2
Electron Beam Gun 1

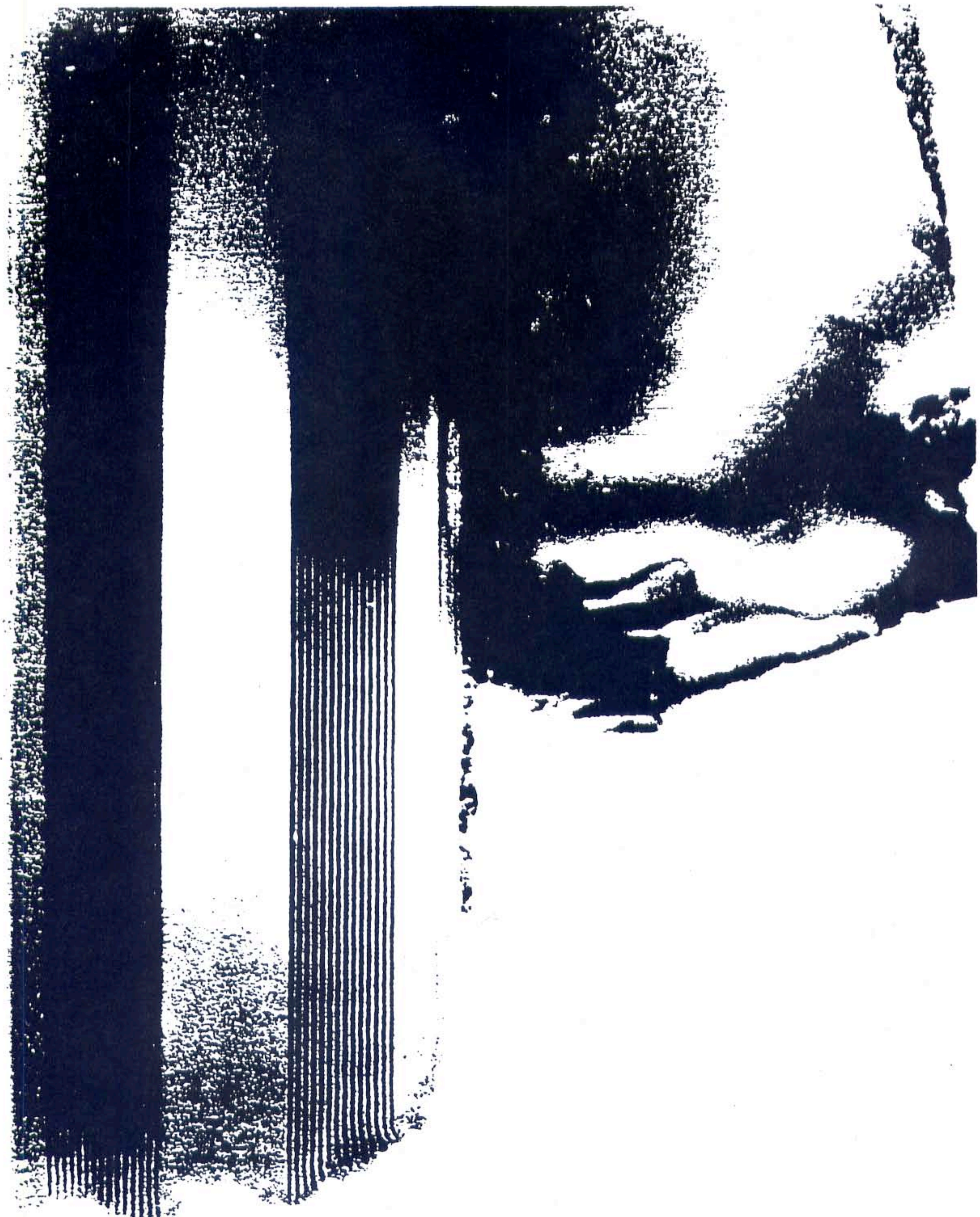

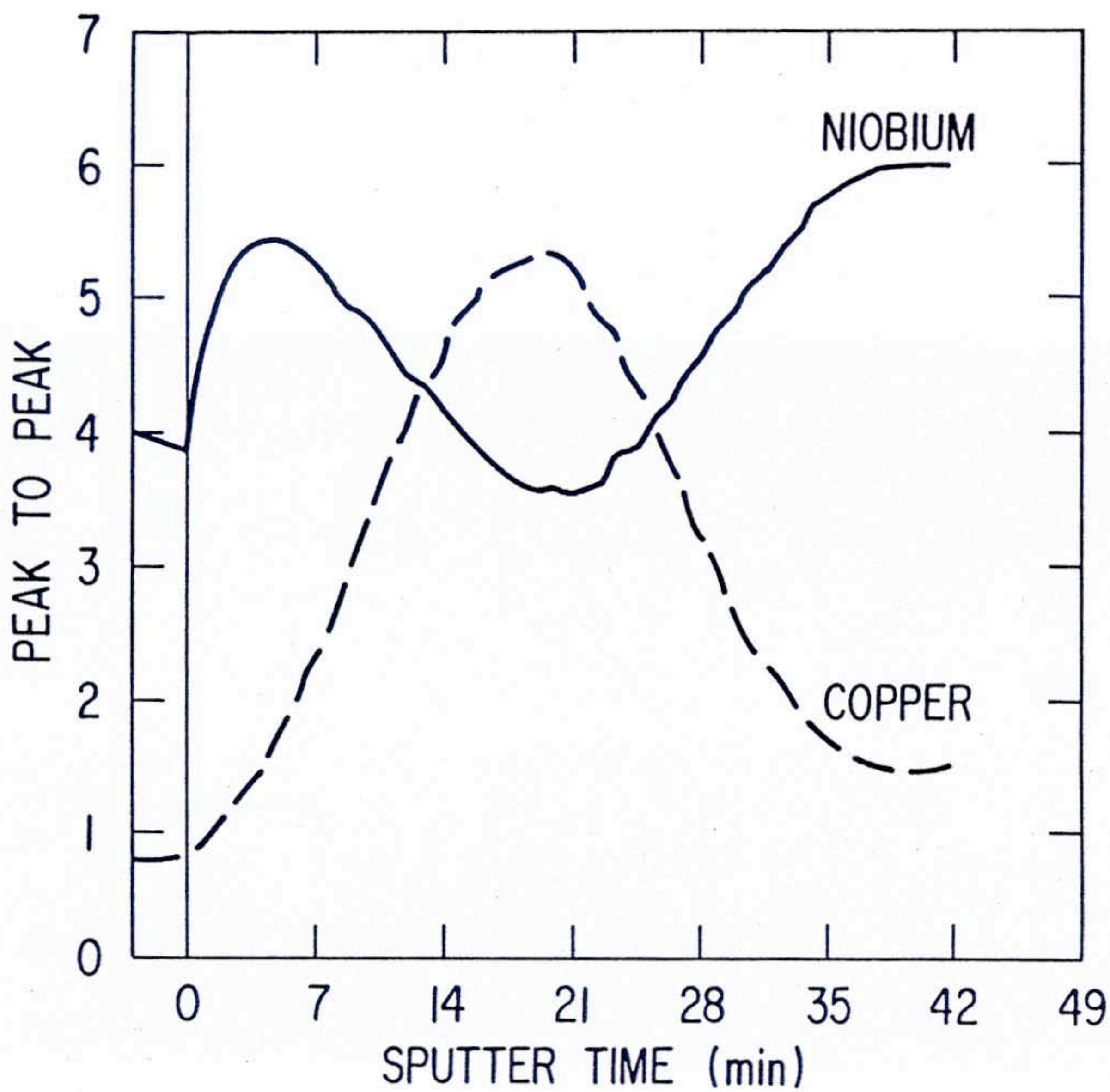

NIOBIUM
COPPER
PEAK TO PEAK
0
1
2
3
4
5
6
7
0
7
14
21
28
35
42
49
SPUTTER TIME (min)

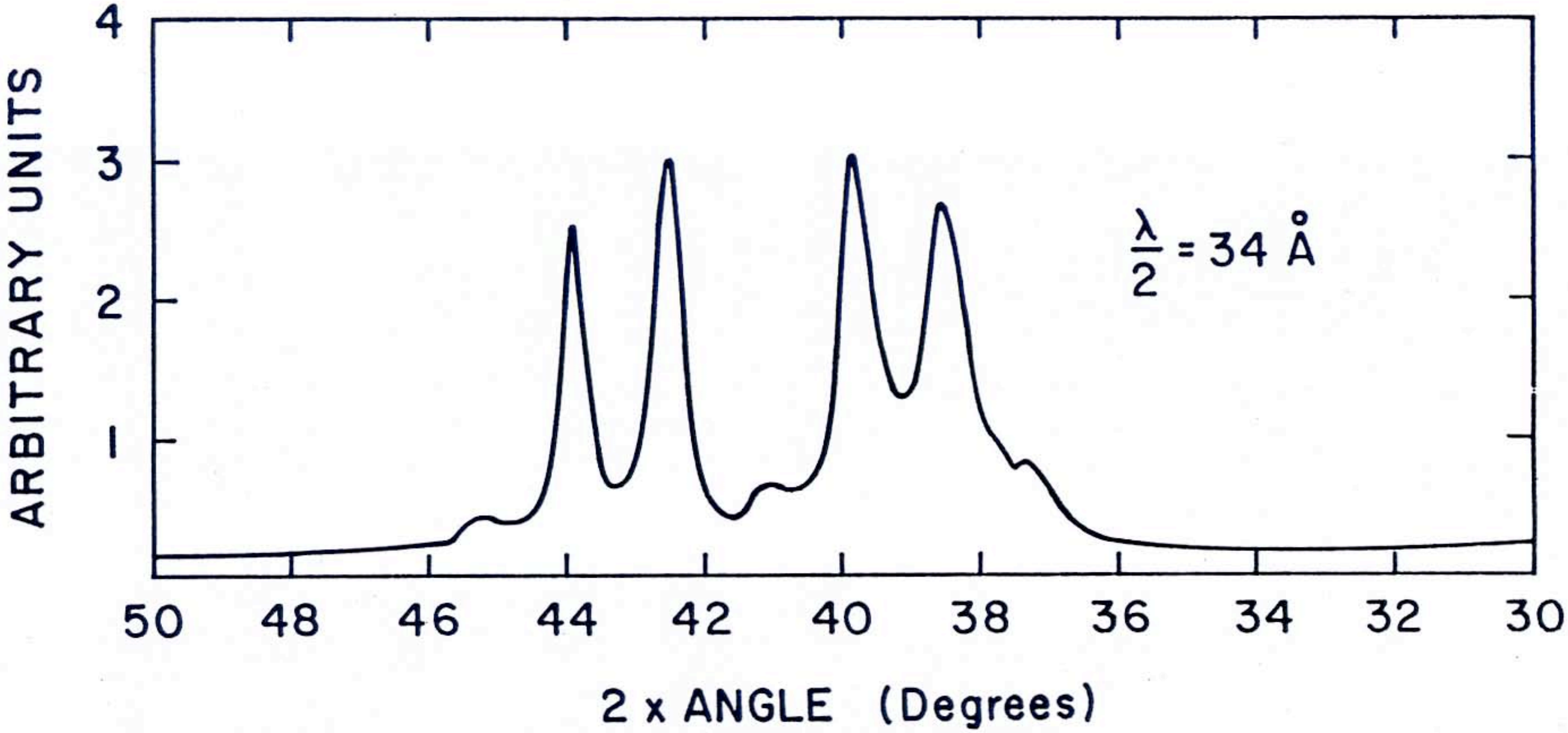

4
3
2
1
ARBITRARY UNITS
λ/2 = 34 Å
50
48
46
44
42
40
38
36
34
32
30
2 x ANGLE (Degrees)

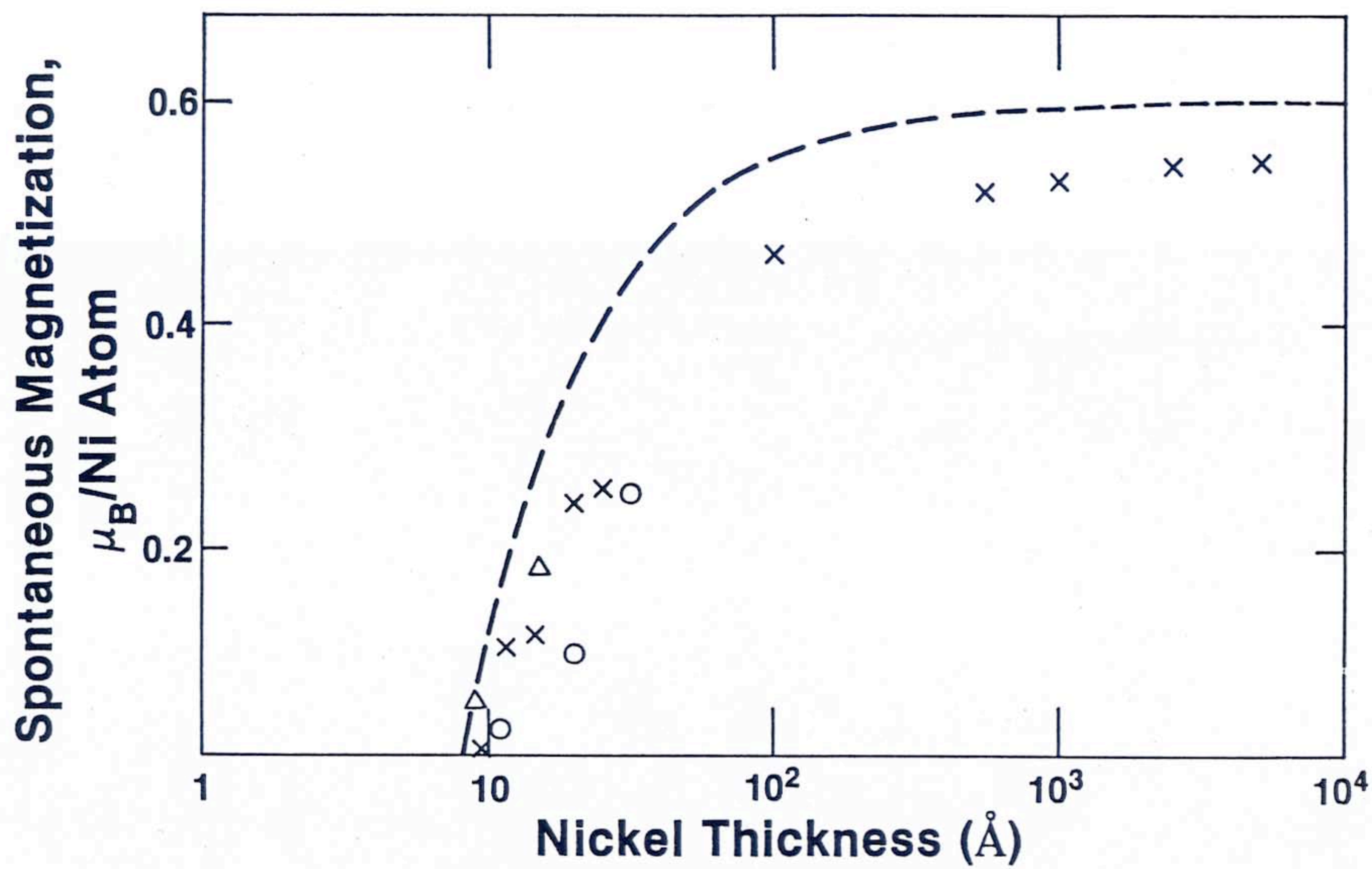

Spontaneous Magnetization,
μB/Ni Atom
0.6
0.4
0.2
1
10
10²
10³
10⁴
Nickel Thickness (Å)

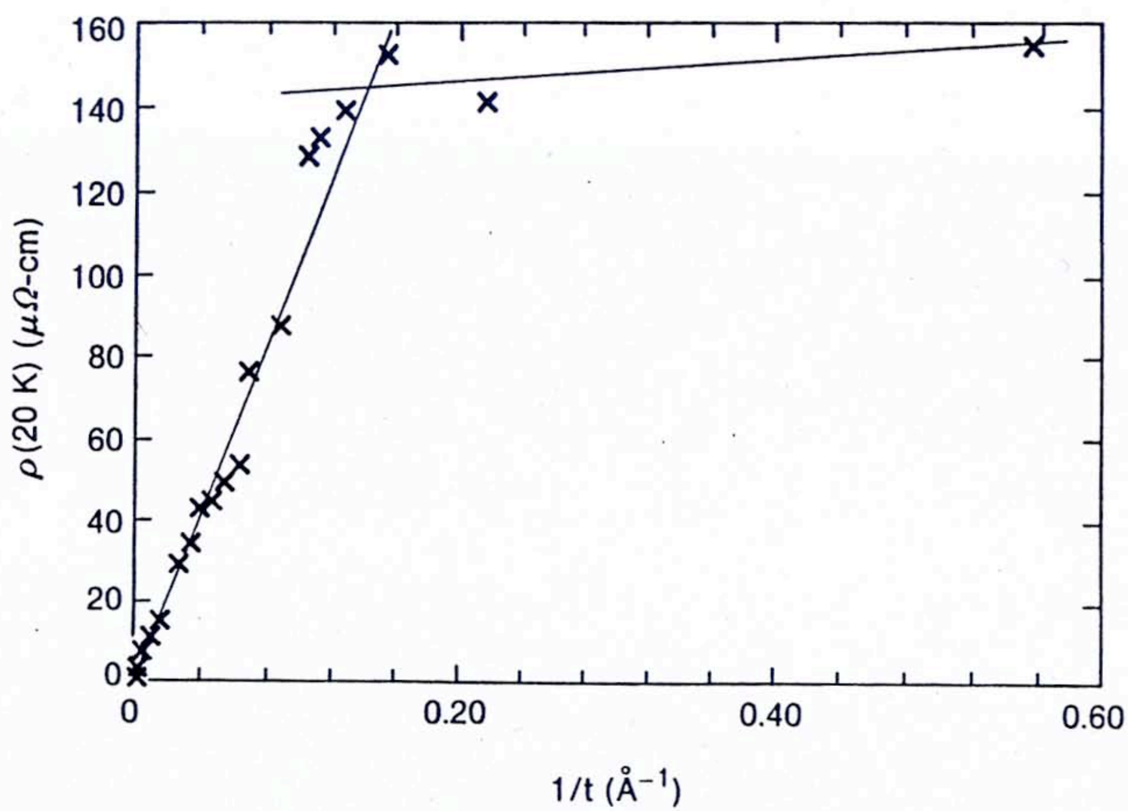
160
140
120
100
80
60
40
20
0
ρ(20 K) (μΩ-cm)
0
0.20
0.40
0.60
1/t (Å⁻¹)

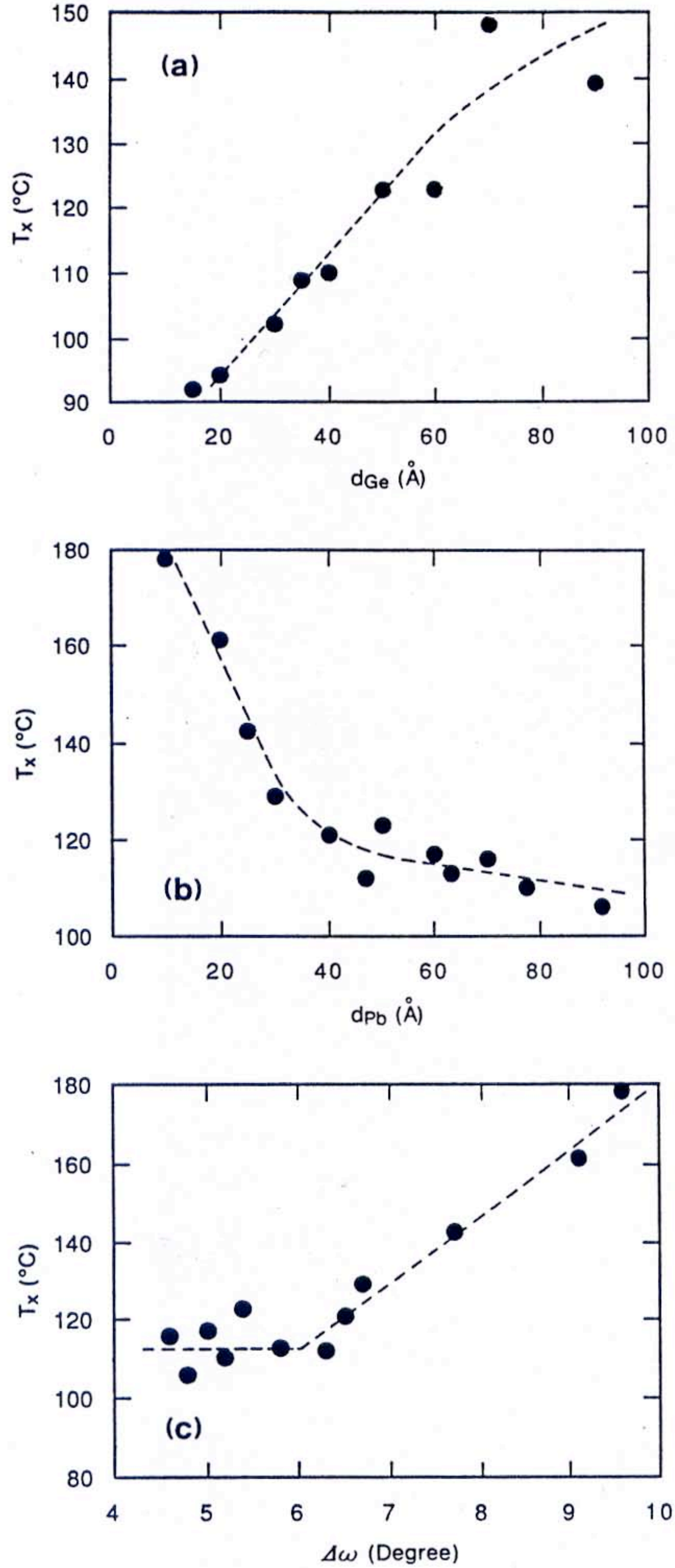
(a)
(b)
(c)
T_x (°C)
d_{Ge} (Å)
d_{Pb} (Å)
$\Delta\omega$ (Degree)
150
140
130
120
110
100
90
180
160
80
0
20
40
60
80
100
4
5
6
7
8
9
10

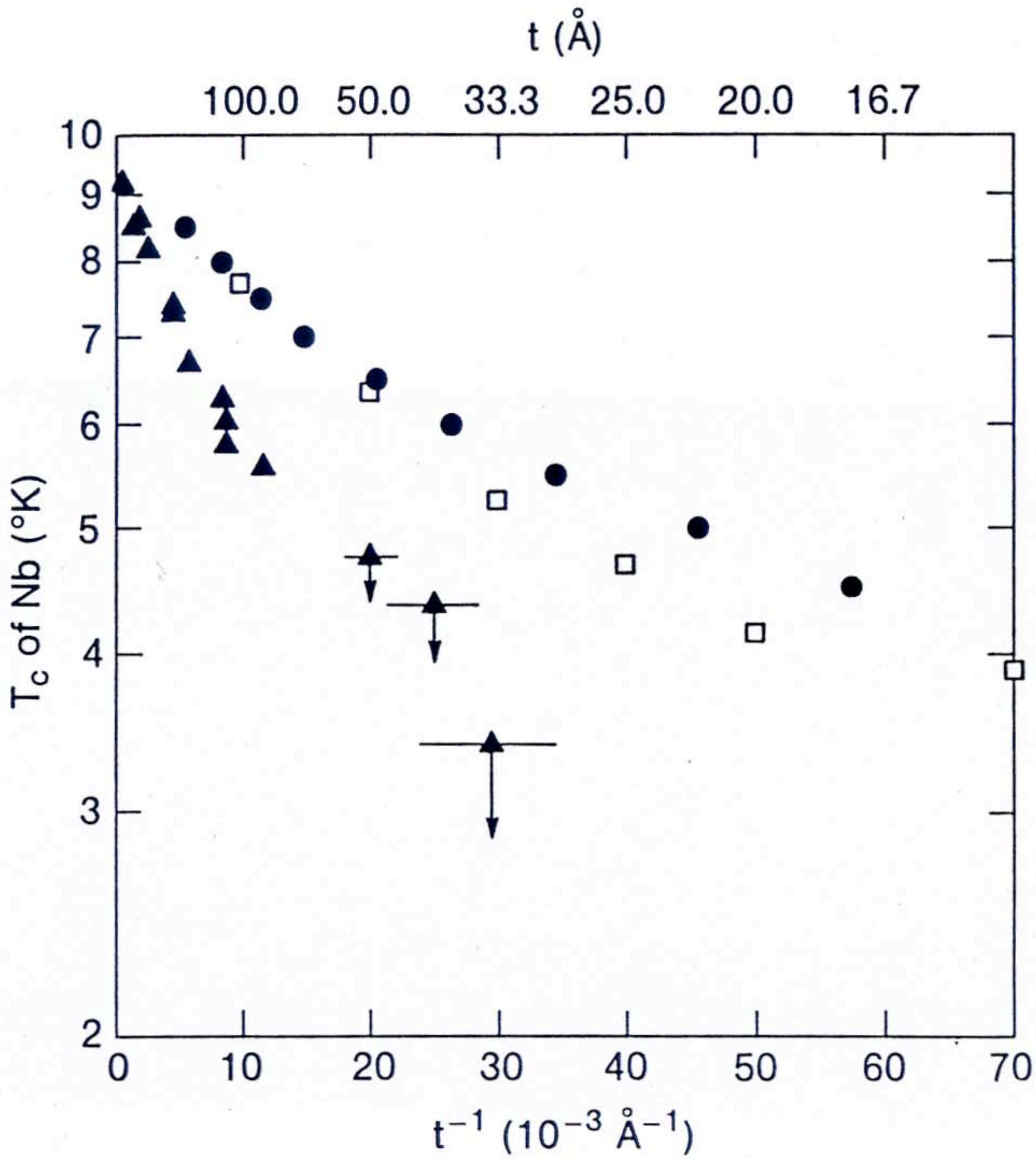

t (Å)
100.0
50.0
33.3
25.0
20.0
16.7
10
9
8
7
6
5
4
3
2
Tc of Nb (°K)
0
10
20
30
40
50
60
70
t−1 (10−3 Å−1)

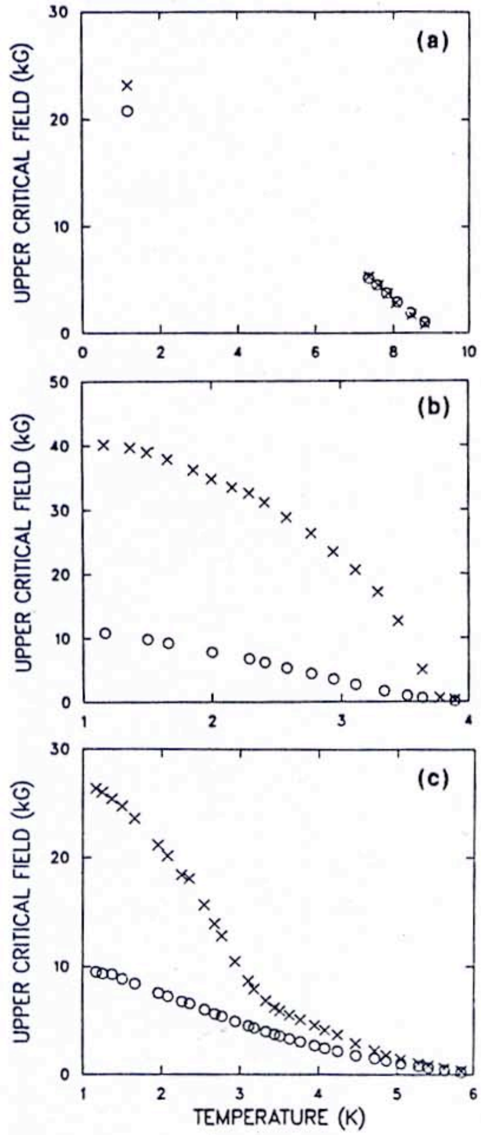

(a)
(b)
(c)
UPPER CRITICAL FIELD (kG)
TEMPERATURE (K)

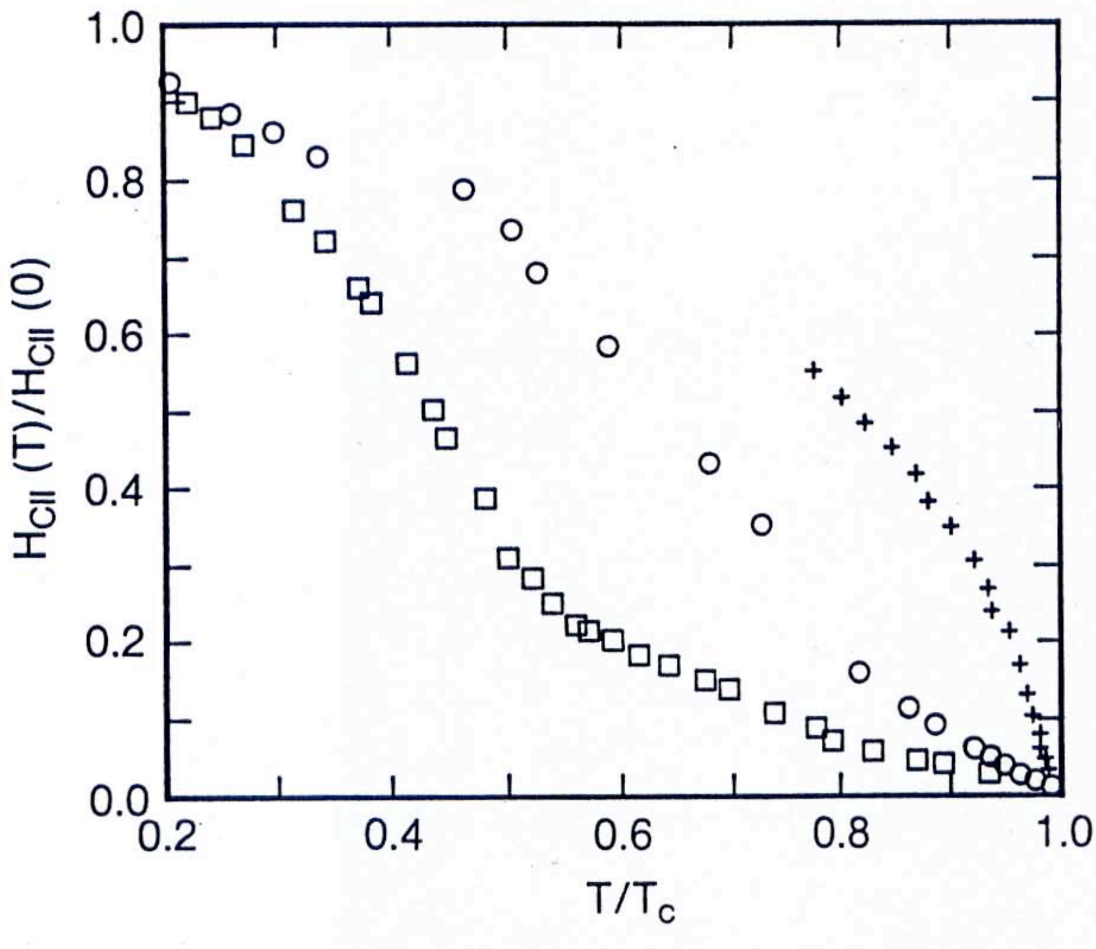

1.0
0.8
0.6
0.4
0.2
0.0
$H_{CII}(T)/H_{CII}(0)$
0.2
0.4
0.6
0.8
1.0
T/T_c

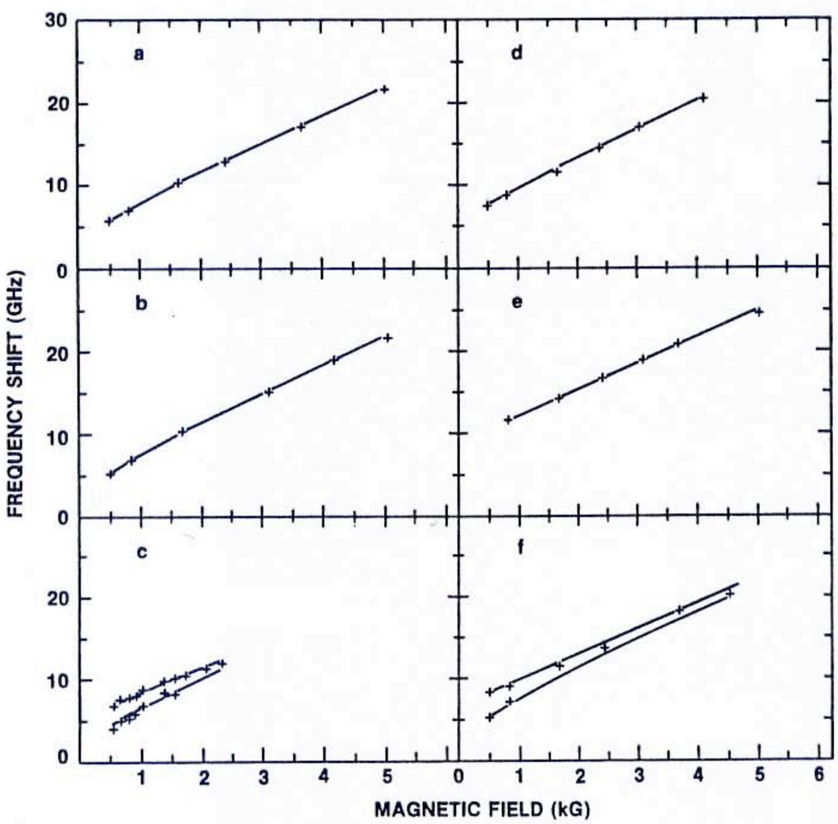
FREQUENCY SHIFT (GHz)
MAGNETIC FIELD (kG)
a
b
c
d
e
f
0
10
20
30
1
2
3
4
5
6

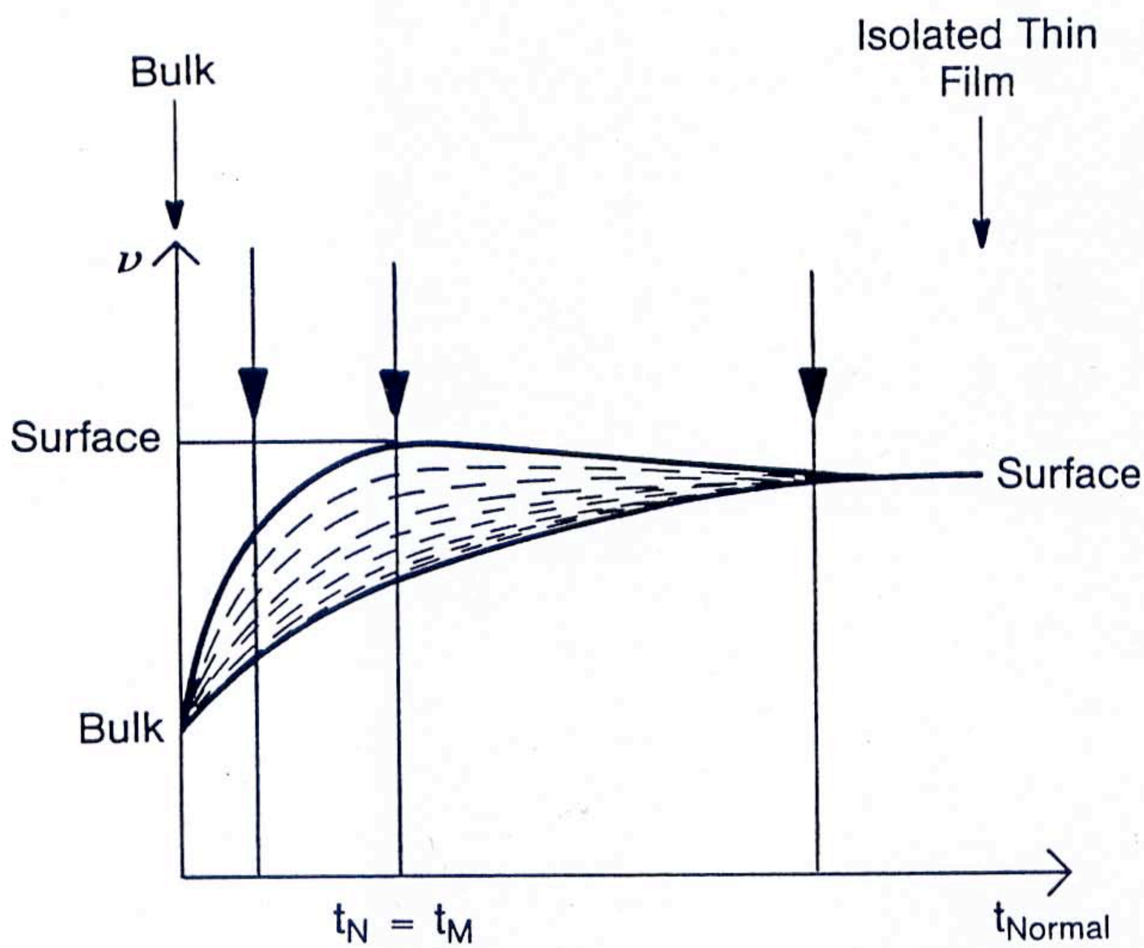

Bulk
Isolated Thin Film
ν
Surface
Surface
Bulk
t_N = t_M
t_Normal